RSC Advances

PAPER

View Article Online
View Journal | View Issue

Cite this: *RSC Adv.*, 2025, **15**, 43293

Determining trace amounts of zinc in environmental and biological samples using solid-phase spectrophotometry

Fahad M. Alminderej,[a] Muneera Alrasheedi,[a] Alaa M. Younis,[a] Alaa S. Amin *[b] and Hesham H. El-Feky[b]

An eco-friendly analytical system utilizing solid-phase spectrophotometry is established for zinc quantification in environmental and biological samples. This method involves sorption of Zn^{2+} as 4-(2-amino-3-hydroxypyridine-4-yl-azo)1,5-dimethyl-2-phenyl-1,2-dihydro-pyrazol-3-one (AHDDO) onto Dowex 1-X8 type anion-exchange resin. The influence of various analytical factors like sample volumes, quantity of AHDDO and pH of the aqueous solution was examined. Direct absorbance assessments of the gel, contained within a 1.0 mm cuvette, were recorded at wavelengths of 640 and 795 nm. The calculated molar extinction coefficients were 3.91×10^7 for 500 mL and 9.78×10^7 L mol^{-1} cm^{-1} for 1000 mL. A linear calibration curve was obtained within the range 20–2250 ng mL^{-1} with RSD of >2.55 ($n = 10$). Employing 50 mg ion-exchange material, the quantification and detection limits were 50 and 15 ng mL^{-1} for 500 mL sample and 20 and 6.0 ng mL^{-1} for 1000 mL sample, respectively. Expanding the volume of the sample may improve sensitivity. The presence of other examined anions and cations showed no notable interference in the quantification of Zn^{2+}. The suggested SPS system was utilized for assessing Zn^{2+} in environmental and biological specimens. The outcomes were evaluated against those acquired through FAAS, confirming the method's validity.

Received 28th August 2025
Accepted 27th October 2025

DOI: 10.1039/d5ra06441d

rsc.li/rsc-advances

1 Introduction

Zinc ranks as the second most prevalent trace element within humans and is vital for numerous enzymatic activities. It is fundamental in processes like spermatozoa production and movement, thereby having a direct impact on the quality and viability of semen.[1,2] Therefore, its detection may be utilized as an indicator of male infertility[3,4] and for forensic examinations.[5] Forensic analysis of semen typically involves examining the prostate-specific antigen (PSA) and the enzyme acid phosphatase (AP).[6] Nevertheless, these techniques may have limitations resulting from the denaturation of bio-macromolecules, interference from certain substances, or AP activity originating from external sources[7,8]

Zinc, an essential micronutrient involved in various physiological functions, contributes to enzyme activity, cell death (apoptosis) regulation, gene transcription, and neural communication.[9] A lack of zinc may hinder neurological development in children and is potentially involved in triggering degenerative brain disorders in adults. Conversely, excessive zinc intake can result in health complications such as anemia and impaired reproductive function.[10] In aquatic environments, even slight decreases in zinc levels may restrict phytoplankton development and reduce the absorption of carbon dioxide.[11] The World Health Organization (WHO) established 0.005 mg mL^{-1} as a maximum allowable concentration of zinc in potable water, underscoring the critical need for precise monitoring of zinc levels in environmental and medical settings.[12–14]

Zinc (Zn) serves as a natural catalyst and plays a vital role as a key indicator in numerous metabolic functions, including hormonal synthesis and genetic regulation. Moreover, Zn^{2+} is actively involved in the metabolic pathways of carbohydrates, proteins, and lipids such as cholesterol.[15] Owing to its scientifically established importance, the advised daily zinc intake is 11 and 8 mg for adult men and adult women, respectively.[16] Worldwide, zinc deficiency poses a significant health issue, impacting millions of people, especially in less developed nations across South and Southeast Asia, Sub-Saharan Africa, Central America, and the Andean regions of South America.[17,18] Insufficient zinc levels within a population primarily result from poor dietary consumption and limited food security. To address this public health challenge, various approaches have been adopted, such as dietary zinc supplements, zinc enrichment of foods, and zinc bio-fortification of agricultural staples.[19]

Because of the increased level of Zn^{2+} in the environment. Multiple analytical approaches comprising atomic absorption

[a]*Department of Chemistry, College of Science, Qassim University, Buraidah, 51452, Saudi Arabia*

[b]*Chemistry Department, Faculty of Science, Benha University, Benha, Egypt. E-mail: asamin2005@hotmail.com*

spectroscopy (AAS),[20,21] flame atomic spectroscopy,[22,23] inductively coupled plasma mass spectrometry (ICP-MS),[24] inductively coupled plasma atomic emission,[25,26] micro-probe X-ray,[22] anodic stripping voltammetry,[26,27] fluorescence analyses,[26] chemiluminescence analysis,[28] ISE[29] or electro analytical techniques.[23,27,29] These approaches have been extensively utilized for detecting heavy metals, even at trace levels. Nevertheless, they tend to be costly and challenging to implement. Although they provide very low detection limits, such techniques can be time-consuming, expensive, and vulnerable to interference from the sample matrix.[30] Compared to other techniques, spectrochemical methods are often favored because they are more cost-effective, easier to use, and have widely accessible equipment.[31]

Green chemistry, which involves employing chemical principles to prevent pollution,[32] has primarily been utilized in both organic and inorganic synthesis. This approach has facilitated the emergence of novel synthetic approaches, the substitution of hazardous solvents, and the reduction of byproducts.[33] Nonetheless, many existing analytical techniques produce substantial quantities of harmful waste, leading to environmental consequences. Therefore, the advancement of more eco-friendly analytical approaches is highly sought after and should be prioritized by analytical chemists.[32] Waste mass and toxicity constitute critical analytical dimensions, equally essential to other characterization factors.

To improve the sensitivity of spectrophotometric techniques and fully exploit their benefits, solid-phase spectrometry (SPS) has been introduced and utilized to quantify trace analytes across a wide range of sample types.[34–53] This approach relies on directly measuring the reduction in light intensity caused by adsorbent particles, or alternatively, detecting the light they emit. The adsorbent is contained within a transparent chamber, where the analyte from the sample accumulates, forming a visible or fluorescent compound.[36,54]

This research develops a more environmentally friendly analytical method for the selective and sensitive quantification of zinc. The primary objective is to explore the feasibility of employing AHDDO as a reagent for quantifying trace levels of Zn^{2+} using the SPS technique. The optimal conditions for the reaction have been examined. Zn^{2+} ions bind to AHDDO to form a lavender pink colored complex, which is readily adsorbed onto Dowex 1-X8 anion-exchange resin. This interaction forms the foundation of a straightforward, precise, and rapid spectrophotometric technique for determining Zn^{2+} at the nanogram per milliliter level, eliminating the need for a prior preconcentration step. The developed method demonstrates high selectivity, being largely unaffected by common interferences, and has been successfully employed in analyzing a range of environmental and biological specimens compared with the results obtained using FAAS method.

2 Experimental

2.1. Materials and reagents

All trials were accomplished at room temperature. Deionized water was used to dilute both the reagents and test samples. Unless otherwise specified, all chemicals employed were of analytical reagent grade. 4-(2-Amino-3-hydroxy-pyridine-4-ylazo) 1,5-dimethyl-2-phenyl-1,2-dihydro-pyrazol-3-one (AHDDO) was formulated according to earlier recommendations.[55] A 5×10^{-3} M solution was formulated through dissolving a proper quantity within 10 mL of ethanol, transferring it to a 100 mL volumetric flask, and then diluting to the mark with ethanol.

Standard Zn^{2+} ion solution 5×10^{-3} M, was formulated through dissolving 1.4372 g $ZnSO_4 \cdot 7H_2O$ (Merck) within distilled water, adjusting the ultimate volume to 100 mL. The solution's concentration was then verified through titration with EDTA.[56] Lower-concentration standard solutions were obtained through proper stock solution dilution.

DEAE-Sephadex® A-25, Amberlite™ MB20, the chloride form of Dowex 1-X8 anion exchange resin (200–400 mesh, sourced from Aldrich), sodium polystyrene sulfonate (SPS Kayexalate, 600 mesh), patiromer (Veltassa, size of ≈100 μm and pore size of 3.0 Å), and sodium zirconium cyclosilicate cation exchange resin (Lokelma with particle size distribution profile of >3.0 μm and pore size of 3.0 Å) {Sigma-Aldrich product} were used in the experiment. Before use, the resins underwent an extensive cleaning process with deionized water, followed by a 5-hour treatment with 2.0 M hydrochloric acid. Subsequent washing continued with water until no chloride ions were detected in the rinse. Once dried in air, the resin was kept in a polyethylene container. Additionally, Thiel buffer solutions of pH 2.5–11.5 were prepared[57] by mixing different proportions of two successive solutions in the following list to obtain the required pH value: 0.05 M oxalic acid + 0.20 M boric acid (*a*), 0.20 M boric acid + 0.05 M succinic acid + 0.05 M sodium sulfate (*b*), 0.05 M sodium tetraborate (*c*), and 0.05 M sodium bicarbonate (*d*), resulting in *a* + *b* (pH 1.5–2.5), *b* + *c* (pH 3.0–9.0), and *c* + *d* (pH 9.5–12.0).

2.2. Instruments used

A glass–calomel combination electrode attached to an Orion Research Model 601A digital ion analyzer was employed to calibrate and confirm the buffer solutions pH. For atomic absorption spectroscopy, a Shimadzu model 670 spectrometer with flame atomization was utilized, with settings adjusted following the manufacturer's recommendations. Atomic absorption was measured employing a nitrous oxide–acetylene flame. A JASCO V-670 UV-Vis spectrophotometer (Tokyo, Japan) recorded the spectral data and absorbance values. To perform absorbance measurements, the sensor membrane specimens were put within a quartz cuvette.

2.3. Absorbance assessments

The absorbance of the reaction-derived compound attached to the ion-exchange resin was determined using a 1.0 mm cuvette at wavelengths of 640 nm and 795 nm. The 795 nm wavelength was specifically chosen because it lies in a spectral region where only the exchanger contributes to light absorption. Measurements were taken relative to a reference 1.0 mm cuvette densely filled with a water-saturated exchanger. The absorbance was measured at the same wavelengths using a cell (1.0 mm)

containing resin pre-treated with the blank solution. This baseline absorbance arises from the reagent bound to the ion-exchange material. The complex's net absorbance (A_{NC}) was determined using the subsequent formula.[58]

$$A_{NC} = A_{complex} - A_{blank}$$

where $A_{blank} = A_{640}/A_{795}$ (for blank) and $A_{complex} = A_{640}/A_{795}$ (for the sample).

2.4. General experimental procedure

(A) For each 100 mL sample, a proper amount containing between 100 and 2250 ng mL^{-1} of Zn^{2+} was measured and poured in a polyethylene container (1.0 L). Subsequently, 2.0 mL of 5×10^{-3} M AHDDO, 10 mL of Thiel buffer adjusted to pH 3.5, and a quantity of an ion exchanger ranging from 25 to 100 mg provides were introduced after the total volume was adjusted to 100 mL. The mixture underwent mechanical agitation at 4500 revolutions per min for a duration of 10 minutes. The resulting colored resin after preconcetration beads were then isolated *via* vacuum filtration and subsequently transferred—using a small pipette—to a cell (1.0 mm) along with a minor quantity of the filtrate. This cell underwent 2.0-minute centrifugation at 4500 rpm. A control solution encompassing all reagents excluding Zn^{2+} ions was similarly formulated and processed under identical conditions. The differential absorbance between the test specimen and the control, quantified as previously outlined, serves to determine the net absorbance value.

(B) For each 500 mL sample, a measured amount with 50–1350 ng mL^{-1} of Zn^{2+} ions was poured into a polyethylene container (1.0 L). Following this, 5.0 mL of a 5×10^{-3} M AHDDO solution, 50 mL of Thiel buffer at pH 3.5, and a quantity of an ion exchanger ranging from 25 to 100 mg provides were introduced. The volume was then adjusted to exactly 500 mL. The obtained solution was agitated mechanically at 4500 rpm for 15 minutes, similar to the previously outlined technique.

(C) For each 1000 mL sample, a suitable volume with 20–575 ng mL^{-1} of Zn^{2+} ions was placed in a polyethylene bottle (1.0 L), after which 5×10^{-3} M AHDDO solution (5.0 mL), Thiel buffer (75 mL; pH 3.5), and a quantity of an ion exchanger ranging from 25 to 100 mg provides were introduced, followed by dilution to the final volume. The stirring duration was extended to 20 minutes at 4500 rpm. Other conditions remained consistent as previously described. Calibration curves were prepared in an identical manner using Zn^{2+} solutions with known concentrations.

2.5. Procedure for food specimens

The food specimens examined were sourced from the local marketplace. They were washed and air-dried to avoid any mineral pollution. The dried material was ground into a suitable particle size (mm) using a mortar. To remove organic components, 10 g of finely ground leaf/chili samples or 10 mL of milk was transferred into a silica crucible and subjected to heating. Subsequently, the samples were incinerated for 4.0–5.0 hours at 550 °C using a muffle furnace. The resulting ash was mixed with 10 mL HNO_3 (2.0 M) under heat to ensure complete dissolution and removal of any organic component present, followed by filtration through acid-washed Whatman No. 41 filter paper. The residue was rinsed with the same paper, followed by additional washing with heated water. Filtrate and wash solutions were transferred into a 25 mL volumetric flask, and double-distilled water was introduced until filled to its calibration line.

2.6. Procedure for water samples

The water specimens were gathered in polyethylene bottles that had been pre-cleaned utilizing doubly deionized distilled water to significantly affect the results, detergent, diluted HNO_3, and deionized water. Prior to analysis, the specimens underwent filtration using a 0.45 μm pore-size Millipore cellulose membrane. The samples were placed within polyethylene containers (1.0 L), acidified with 1.0% HNO_3, and then kept refrigerated at 4.0 °C. To remove chlorine from tap water, the specimens underwent a 5.0-minute treatment with activated charcoal (5.0 g), followed by filtration prior to being positioned in a polyethylene bottle. The pH of each sample was then set to 3.5 before analysis.

2.7. Method for zinc in pharmaceutical preparations

2.7.1. Hamoderme (talc powder). A 25 mg sample was combined with 3.0 mL concentrated HNO_3 to completely dissolve. After treatment, the mixture underwent dilution, rinsing with water, and filtration to eliminate the white precipitate. The resulting filtrate along with the rinse solutions were then made up to 250 mL (an ultimate volume). Zinc content in this solution was determined employing the identical analytical procedure used for the 500-mL sample analysis to detect the lower concentration range present.

2.7.2. VitaZinc (capsules) and Stresstabs/600. The capsule underwent dissolution within aqua regia, and the resulting mixture underwent complete evaporation until completely dry. Subsequently, concentrated HNO_3 (2.0 mL) was introduced to the residue to ensure complete dissolution and removal of any degradation product of multivitamins present, followed by evaporation to dryness once more. The procedure was carried out three times before dissolving in deionized water (250 mL). A portion was then extracted to measure the zinc content per capsule, following the prescribed method for a 500-mL sample to define the lower concentration range present.

2.7.3. Prozoline zinc (solution). A 10 mL aliquot of the solution underwent evaporation until dry, after which the soluble salts underwent dissolution within concentrated nitric acid (2.0 mL). The mixture underwent filtration to eliminate the insoluble solids and subsequently underwent three rinses with deionized water. The filtrate volume was adjusted to 50 mL in a volumetric flask. A 10 mL portion was then examined for zinc content adhering to the procedure adopted for the 500 mL sample to determine the lower concentration range present.

2.8. Method for biological samples

The hair specimen was sequentially washed with chloroform, acetone, and double-distilled water, followed by drying at 60 °C.

A precisely measured 0.5 g portion of the sample underwent treatment with concentrated sulfuric acid (3.0 mL) and concentrated nitric acid (30 mL) to complete dissolution and removal of any organic component present, then was subjected to 30-minute heating at 150 °C utilizing a hot plate. Around 25 mL of a 30% H_2O_2 solution was slowly introduced until the mixture became clear. It was then evaporated at 200 °C until only a faint white residue remained, indicating near-complete dryness. Roughly 5.0 mL of a 0.1 M nitric acid was introduced into the beaker, and the mixture was subsequently subjected to 15-minute heating at 100 °C. The solution's pH was brought to 3.5, then diluted to 100 mL in a conical flask. Subsequently, 5.0 mL of this diluted sample was subjected to analysis following the specified protocol for a 500 mL volume to detect the lower concentration range present and the findings were relative to those attained employing the FAAS method.

Employing a closed vessel microwave oven, samples of rat femur, feces, and kidney were prepared. Each sample (approximately 315 mg of kidney, 460 mg of femur, and 114 mg of feces) was carefully weighed (±0.1 mg) and then placed into vessels made of polyfluoroethylene to significantly affect the results. The femur specimen was immersed in concentrated nitric acid for 12 hours prior to microwave digestion. The specimens were combined with HNO_3, transferred into a microwave oven operating under pressure (up to 1.03×10^6 Pa), and subjected to irradiation for 75 minutes at a 100 W maximum power. The solutions obtained were subsequently treated with 30% hydrogen peroxide, followed by transfer to volumetric flasks and dilution using deionized water to the required volume. A measured portion of the sample solution, ranging from 10 to 50 mL, was individually collected. Zinc concentration was then determined using the standard procedure for a 500 mL volume to define the lower concentration range present, and the findings were evaluated against the results from the FAAS technique.

Micro-quantities of Zn in blood serum were measured utilizing the subsequent method: a 3.0 mL sample of serum was placed in a conical centrifuge tube (10 mL), then 2.0 drops of thioglycolic acid were introduced and thoroughly blended. A 3.0 mL volume of 2.0 M HCl was introduced to ensure complete dissolution and removal of any organic component present, followed by adding 0.8 mL of 40% trichloroacetic acid, with thorough mixing following each addition. The mixture underwent thorough stirring using a glass rod for about one minute and was then subjected to centrifugation at 3000 rpm for ten minutes. An appropriate volume of the resulting supernatant was extracted, and the zinc concentration was analyzed following the standard addition method previously outlined for a 500 mL sample to detect the lower concentration range present.

2.9. Method for zinc in meat samples

Meat was obtained from nearby markets, then ground, thoroughly mixed, freeze-dried, and stored within dry, clean containers. Following the sieving process, only particles smaller than 100 μm were selected. A 0.5-gram portion of the sample was combined with HNO_3 within a glass container and subjected to heating utilizing a hotplate for complete dissolution and removal of any organic component present, until it was fully dissolved. After cooling, the solution was moved to a 100 mL volumetric flask, with ultrapure water added to bring the volume to the final mark. The zinc content was subsequently analyzed following the general method outlined earlier based on 500 mL and FAAS to detect the lower concentration range present.

3 Results and discussion

3.1. Absorption spectra in solid phase

AHDDO forms a lavender pink complex when it reacts with Zn^{2+} ions in solution, exhibiting its highest absorbance at 597 nm. The complex displays a 1 : 1 stoichiometric ratio, as verified by both the continuous variation and molar ratio techniques. Within the pH range of 3.0–4.0, the complex is adsorbed completely onto the Dowex 1-X8 anion exchange resin, resulting in an absorption peak shift to 640 nm. Using other anionic and cationic ion exchanges the formed complex adsorbed was leached from these ion exchanges. The adsorbed complex produces a stable, transparent gel that cannot be reversed, making the scattering phenomenon un-measurable. AHDDO is adsorbed onto the resin, exhibiting an orange hue with a peak absorbance at 462 nm (466 nm in solution). Fig. 1 presents the spectra of the complex in both solution and resin states.

3.2. Optimisation of variables

3.2.1. pH dependence. This parameter was demonstrated through the implementation of both 500 mL and 1000 mL methods. The ideal pH range for species generation and stabilization was between 3.0 and 4.0 (Fig. 2). Absorbance showed a marked decline at pH levels lower than 3.0 and higher than 5.0. Various buffer systems (including phosphate, acetate, borate, Thiel, and universal buffers) were assessed to determine the most suitable buffering medium. The most effective

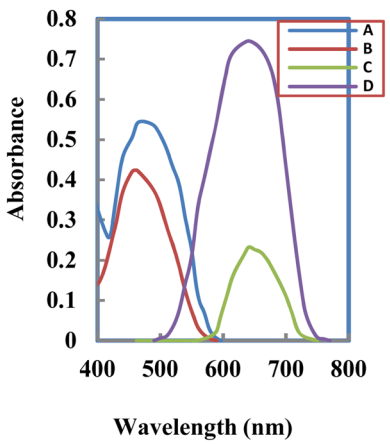

Fig. 1 Absorption spectra of (A) blank in solution (B) blank for SPS, (C) SPS for 500 mL and (D) SPS for 1000 mL samples for 500 ng per mL Zn^{2+}.

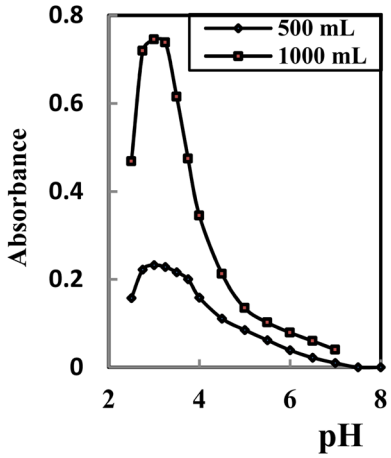

Fig. 2 Effect of pH on fixation and complexation of 500 ng mL^{-1} of Zn^{2+} ions for 500 and 1000 mL samples using 50 mg of Dowex 400 mesh.

outcome was achieved using a Thiel buffer of pH 3.5. Absorbance remained unaffected by ionic strength, which was adjusted using the buffer solution, at concentrations up to 0.05 M. At elevated concentrations, the absorbance rapidly declined, as commonly observed in SPS research, likely due to the anions in the buffer competing for the resin's anionic binding sites.

3.2.2. Reagent concentration. Absorbance rises in proportion to the AHDDO concentration, continuing up to a molar ratio of [AHDDO]/[Zn^{2+}] exceeding 10 (for 100 mL sample). Therefore, 2.0 mL of 5×10^{-3} M AHDDO was chosen for 100 mL, whereas. 5.0 mL of 5×10^{-3} M AHDDO were chosen for 500 and 1000 mL procedures, because the findings show strong agreement at such concentrations.

3.2.3. Other experimental conditions. The sequence in which reagents were added did not influence the outcome, and the order followed here was sample–AHDDO–buffer–resin. As expected, increasing the resin mass (m_r, in g) resulted in a decrease in absorbance readings.[59] The ideal stirring time was 10, and 15 min for 100 and 500 mL samples and 20 min for a 1000 mL sample (Fig. 3). The stabilized species remained unchanged for no less than 8.0 hours following equilibration. Analysis of solvent influence indicated that the solvent had no impact on the course of the reaction. An increase in ethanol concentration does not influence the absorbance of the resulting complex. Likewise, varying the ionic strength (μ) has no noticeable impact on the complex matrix's absorbance, suggesting that the complexation mechanism operates independently of ionic strength.

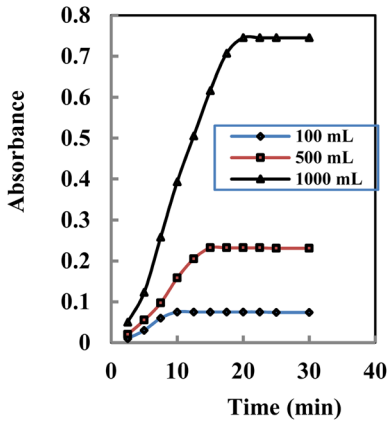

Fig. 3 Effect of shaking time on fixation of complex of 500 ng per mL Zn^{2+} for 100, 500 and 1000 mL samples using 65, 50, and 50 mg, respectively, of Dowex1-X8 (400 mesh).

The consistency of the process is enhanced when the cells containing the solid phase are subjected to centrifugation prior to conducting spectrophoto-metric analysis. Increasing the quantity of ion exchanger resulted in a decrease in the amount of species adsorbed, which lowered absorbance; conversely, using too little may lead to handling or operational challenges.

However, varying the amount of an ion exchanger ranging from 25 to 100 within this interval enables the optimization of methods with differing levels of sensitivity. Unless specified otherwise, all measurements were performed using 50 to 70 mg of exchanger, striking a balance between high sensitivity and practical ease of use.

The least quantity of dry resin necessary to occupy the cell and allow for easier management, *i.e.* 65, 50 and 50 mg, was employed for 100, 500 and 1000 mL samples, correspondingly, for all measurements. The absorbance decline was described by the empirical formula $A_c m_r^{0.745} = 0.049$. When absorbance A_c is denoted against $1/m_r$, we represented that absorbance diminished as described by the formula $A_c = 0.014 + 0.047/m_r$ ($r = 0.999$). The correlation between the slope and molar absorption can be calculated as follows:[60]

$$A_c = \frac{\varepsilon_c L_R C_0 V 100}{m_r + V/D}$$

In this equation, m_r is the mass of ion exchanger (g), D denotes the distribution ratio (L g^{-1}), C_o is the initial concentration of Zn^{2+} (M), V denotes the sample solution volume (L), L_R the mean light-path length through the solid phase (cm), and ε_c is the sample species molar absorptivity in the ion-exchanger phase (1.60×10^4 kg mol^{-1} cm^{-1}). In the suggested method, the term V/D can be considered negligible relative to m_r due to the large value of D. As a result, the simplified expression linking absorbance to the ion-exchanger mass is obtained:

$$A_c = \frac{\varepsilon_c L_R C_0 V 1000}{m_r} = \frac{K}{m}$$

where $\varepsilon_c L_R C_o V 1000$ is the slope obtained from plotting A_c *versus* $1/m_r$. Assuming L_R/0.1 cm, the calculated value for $K = 1.6 \times 10^4 \times 0.1 \times 2.94\ 10^{-7} \times 0.1 \times 1000 = 0.048$, this aligns well with the experimental value of 0.046.

3.3. Nature of the fixed complex

The stable Zn^{2+}–AHDDO complex bound to Dowex 1-X8 resin was investigated at the pH 3.5 employing the Job's continuous variation and molar ratio approaches. By altering the concentration of AHDDO, the graph of A against the [AHDDO]/[Zn^{2+}]

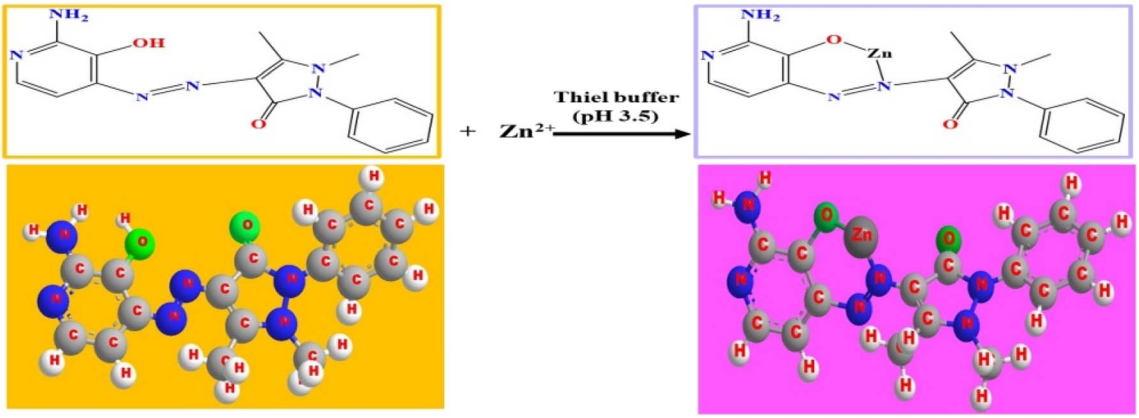

Scheme 1 The complexation of AHDDO with Zn^{2+} ions and the formed Zn–AHDDO complex.

molar ratio exhibited a distinct inflection point at a 1 : 1 ratio, suggesting the formation of a stable complex containing one AHDDO molecule. Furthermore, the Job's process demonstrates a ratio [AHDDO]/[Zn^{2+}] 1.0. As a result, the findings confirmed a stoichiometric proportion of 1 : 1 between [AHDDO] and [Zn^{2+}], consistent with values observed in aqueous solution. AHDDO can function as a bidentate ligand, featuring two donor atoms positioned within the same plane. Lastly, by examining the FTIR spectra of both AHDDO and the AHDDO–Zn complex, the scientists successfully proposed a structural model for the complex, as illustrated in Scheme 1.

The metal ion forms coordination bonds with both the azo-linked nitrogen and the hydroxyl group adjacent to the aromatic ring in the AHDDO structure. The structural and morphological characterization of the modified sorbent was made using FTIR and SEM to better support the zinc adsorption mechanism. Consequently, the overall mechanism of complex formation and stabilization can be represented by the equation below:

$$Zn^{2+} + HL + X^- \rightleftarrows ZnLX + H^+ \text{ (complexation process)}$$

$$ZnLX + Cl_m{}^-R^{m+} \rightleftarrows ZnLXCl_{m-1}{}^-R^{m+} + Cl^- \text{ (fixation process)}$$

$$Zn^{2+} + HL + X^- + Cl_m{}^-R^{m+} \rightleftarrows ZnLCl_{m-1}{}^-R^{m+} + Cl^- + H^+ \text{ (global process)}$$

where X denotes a dentate anion (Cl^-, CH_3COO^-) that occupies the sixth coordination site of the zinc ion, and $Cl_m{}^-R^{m+}$ represents the anionic resin.

3.4. Effect of foreign ions

A comprehensive analysis was conducted on the interference effects of various cations and anions, in quantities spanning up to 10 mg, with 500 ng mL^{-1} of zinc. The interference tolerance level was defined as the concentration of competing ions that caused a deviation exceeding ±5.0% in the absorbance measurement of a fixed Zn^{2+} concentration. This threshold, commonly known as the tolerance limit,[61,62] was determined by measuring the membrane's absorbance before and after introducing a specific concentration of interfering ions into a 100 ng mL^{-1} Zn^{2+} solution. The obtained results are presented in (Table 1).

To assess selectivity, the effect of various interfering ions on Zn^{2+} detection absorbance was examined. The relative error (RE), indicating the influence of these interfering ions, was calculated using the formula:

$$RE\ (\%) = [(A - A_0)/A_0] \times 100,$$

where A represents the absorbance in the presence of interfering ions, and A_0 is the baseline absorbance without interference.

Table 1 Tolerance ratio (TR = ion/Zn^{2+} mass ratio) for different interfering ions in the measurement of 500 ng per mL M of Zn^{2+a}

Ion	TR	RE%	Ion	TR	RE%
Li^+, K^+, acetate	20 000	−2.6	Fe^{3+}, Al^{3+}, $CO_3{}^{2-}$	5500	+4.5
Ag^+, Na^+, Tl^+, citrate	18 000	+2.9	Fe^{2+}, oxalate	4500	+3.8
Ca^{2+}, Sr^{2+}, succinate	16 500	+3.7	Ni^{2+}, Pd^{2+}, $SO_4{}^{2-}$	3750	+4.4
Mg^{2+}, Ba^{2+}, $NO_2{}^-$, $NO_3{}^-$	15 000	+3.1	Co^{2+}, Hg^{2+}, $HCO_3{}^{2-}$	3000	+3.5
Ti^{4+}, Se^{4+}, Ge^{4+}, $PO_4{}^{3-}$	13 500	−3.8	Sn^{2+}, Pb^{2+}, Cl^-	2500	−4.2
Mn^{2+}, Bi^{2+}, $IO_3{}^-$	12 000	−3.3	Sn^{4+}, Zn^{2+}, SCN^-	2000	+3.4
Th^{4+}, Zr^{4+}, $S_2O_3{}^{2-}$	10 000	+3.6	La^{3+}, Au^{3+}, Cr^{3+}	1500	+4.7
W^{6+}, Mo^{6+}, Br^-	8500	−3.8	Pt^{4+}, Te^{4+}	1000	+4.6
Cr^{6+}, $UO_2{}^{2+}$, $B_4O_7{}^{2-}$	7000	+3.9	Cd^{2+b}, Cu^{2+c}	500[b]	+4.8

[a] TR: tolerance limits; RE: relative error. [b] 1.0 mL of 0.5% thiocyanate solution. [c] 1.0 mL of 0.3% oxalate solution.

Table 1 displays the tolerance limits and the relative error for the ions examined. Cu^{2+} and Cd^{2+} were the most interfering species due to their ability to bind with AHDDO, forming solid-phase complexes that absorb at the detection wavelength. The interference from Cu^{2+} can be mitigated by adding 1.0 mL of an oxalate solution (0.3%) as a masking agent. Similarly, Cd^{2+} interference can be eliminated using 1.0 mL of a 0.5% thiocyanate solution, increasing the tolerance limit by 500 times its excess concentration. Hence, it can be concluded that the suggested approach demonstrates adequate selectivity.

3.5. Quantification

Table 2 displays an overview of the analytical parameters. It was confirmed that a significant portion of the relative standard deviation (RSD) originates from the inconsistency in how the ion-exchanger is packed. For a 100 mL sample analyzed through eight replicate measurements without centrifugation, the RSD was 6.35%. After centrifuging for 2.0 minutes at 4500 rpm prior to measuring absorbance, the RSD dropped to 2.55%, while absorbance readings increased by approximately 15%. Although the same amount (50 mg) of ion-exchange material as optimum, results in different detection and quantification limits for the 500 mL and 1000 mL sample is due to different stirring times of 15 and 20 min for 500 mL and 1000 mL sample, respectively. The quantification limit (QOD) = $3S_B/m$ and detection limit (LOD) = $10S_B/m$ (where S_B and m are blank's standard deviation and calibration graph's slope, respectively),[63] were assessed for every sample system (Table 2). The detection limit of the technique proposed is evaluated compared to those documented for spectrophotometric

Table 2 Analytical characteristics of calibration curve

	Sample volume					
Parameter	100 mL		500 mL		1000 mL	
Amount of exchanger (mg)	50	65	50	65	50	65
pH	3.5	3.5	3.5	3.5	3.5	3.5
Optimum [AHDDO] (M)	1.0×10^{-4}	1.0×10^{-4}	5.0×10^{-5}	5.0×10^{-5}	2.5×10^{-5}	2.5×10^{-5}
Stirring time (min)	10	10	15	15	20	20
Beer's range (μg mL^{-1})	0.25–11.7	0.1–2.25	0.05–1.35	0.15–8.16	0.02–0.575	0.1–1.79
Ringbom range (μg mL^{-1})	0.75–10.8	0.25–2.00	0.15–1.20	0.30–7.90	0.1–0.550	0.30–1.55
Molar absorptivity (L mol^{-1} cm^{-1})	4.14×10^5	7.82×10^6	3.91×10^7	2.81×10^6	9.78×10^7	3.15×10^6
Sandell's sensitivity (ng cm^{-2})	0.0056	0.0012	0.0008	0.0038	0.0005	0.0022
Intercept	−0.009	0.005	0.007	−0.011	−0.004	0.010
Slope (ng mL^{-1})	0.15	0.04	0.43	0.18	1.50	0.69
Correlation coefficient (r)	98.75	99.25	99.67	99.10	99.85	99.50
Detection limit (ng mL^{-1})	75.0	30.0	15.0	25.0	6.00	10.0
Quantification limits (ng mL^{-1})	250	100	50.0	80.0	20.0	35.0
RSD (%)	6.15	2.55	2.25	5.78	1.90	5.25

Table 3 Selectivity and sensitivity of reagents employed for the spectrophotometric measurement of zinc

Reagent	λ_{max} (nm)	ε, L mol^{-1} cm^{-1}	LOD μg mL^{-1}	Interference	Ref.
1-(2-Thiazolylazo)-2-naphthol	590	2.02 × 105	2.02	Cu^{2+}, Co^{2+} and Ni^{2+}	39
1,3-Cyclohexanedionedithiosemicarbazone	570	1.10 × 104	1.42	Fe^{3+}, Al^{3+}, Ni^{2+}, Cu^{2+} and Pb^{2+}	40
1-(2-Pyridylazo)-2-naphthol	560	—	7.30	Fe^{2+} and Fe^{3+}	41
2-(2-Quinolylazo)-5-dimthylaminophenol	590	—	1.22	—	42
Glyoxaldithiosemicarbazone	433	1.42 × 104	1.30	Bi^{3+}, Cd^{2+}, Ni^{2+}, IO^{3-} and BrO^{3-}	43
N-Ethyl-3-carbazolecarboxaldehyde-3-thiosemicarbazone	420	1.55 × 104	1.55	Pb^{2+}, Ni^{2+}, Pd^{2+}, Cu^{2+}, and Cd^{2+}	44
2-(4-Pyridylazo)resorcinol (500 mL)	500		94.0	Pb^{2+}, Mn^{2+}, Cu^{2+}, Cd^{2+}, V^{5+}, Ni^{2+} and Co^{2+}	45
Xylenolorangeandcetylpyridiumchloride	580	2.10 × 104	1.11	Cd^{2+}, Hg^{2+}, Cu^{2+}, Bi^{3+}, Pd^{2+}, Ni^{2+}, Co^{2+} and Ag^{+}	46
Zincon (1000 mL)	621	—	31.0	Co^{2+}, Cu^{2+}, Cd^{2+}, Bi^{3+}, Pb^{2+}, Hg^{2+}, Al^{3+} and Cr^{3+}	47
Nitrilotriacetic acid	550	—	33.0	Fe^{2+}, Co^{2+}, Fe^{3+} and Al^{3+}	48
5-(2-Benzothiazolylazo)-8-hydroxyquinoline (1000 mL)	675	2.50 × 107	6.28	Cu^{2+}, Cd^{2+} and Ni^{2+}	49
1-(2-Pyridylazo)-2-naphthol (2000 μL)	555		50.0	Mn^{2+}, Fe^{3+}, Cu^{2+} and Mo^{6+}	50
1-(2-Tiazolylazo)-2-naphthol	595		25.0	Cu^{2+}, Ni^{2+}, Pb^{2+} and Sn^{2+}	51
AHDDO (500 mL)	640	3.91 × 107	0.15	Cd^{2+} and Cu^{2+}	This work
AHDDO (1000 mL)	640	9.78 × 107	0.006	Cd^{2+} and Cu^{2+}	This work

Table 4 Measurement of Zn^{2+} in food samples

Sample	Zinc found[a]			
	Proposed	FAAS	*t*-Test[b]	*F*-Value[c]
Vegetable samples ($\mu g\ g^{-1}$)				
Potato[d]	53.5 ± 0.06	54.0 ± 0.17	1.37	3.15
Tomato[d]	65.0 ± 0.05	60.5 ± 0.19	1.71	3.47
Carrot[d]	75.0 ± 0.07	61.7 ± 0.22	1.53	3.36
Wheat[c]	34.2 ± 0.04	33.8 ± 0.14	1.42	3.15
Rice[d]	22.8 ± 0.08	23.1 ± 0.23	1.18	2.87
Milk samples ($\mu g\ mL^{-1}$)				
Goat[e]	4.6 ± 0.08	4.7 ± 0.17	1.44	3.06
Sheep[e]	3.0 ± 0.09	3.0 ± 0.20	1.61	3.35
Cow[e]	4.2 ± 0.06	4.1 ± 0.17	1.75	3.64

[a] Means ± standard deviations ($n = 6$). [b] The critical *t*-value ($\alpha = 0.05$, df = 5) = 2.57. [c] The critical *F*-value ($\alpha = 0.05$, df = 5) = 5.05. [d] Gathered from Benha, Egypt. [e] Gathered from Zagazig, Egypt.

techniques found in existing literature (Table 3). The results demonstrate a significant reduction in the quantification and detection limits achieved by the suggested technique, particularly when compared to the solution.[39–51] Comparing the detection limit of the suggested method with that of 2-(4-pyridylazo)resorcinol (500 mL),[43] it was observed that the LOD was approximately 600 times as much as that employing 2-(4-pyridylazo) resorcinol (Table 2), whereas, it is more than ten time as that using *N*-ethyl-3-carbazolecarboxaldehyde-3-thiosemicarbazone.[44] Comparable to the results obtained using 5-(2-benzothiazolylazo)-8-hydroxyquinoline (1000 mL),[49] our technique achieves a lower LOD by 1000 time, while utilizing Zincon (1000 mL),[47] present methodology shows approximately 1000-fold improvement in detection sensitivity. Practically, the relationship between absorbance and sample volume can also be inferred from the gradient of the calibration curves. The sensitivity ratios (S) of the tested specimens are: $S1000/500 = 2.5$; $S1000/100 = 12.5$ and $S500/100 = 5.0$. The theoretically predicted values derived employing the distribution ratio value[62] D are 2.55, 12.40 and 4.95, correspondingly. The variability in baseline absorbance recorded for the blank—determined as the standard deviation from ten replicate measurements—for the 100, 500, and 1000 mL sample volumes was 0.006, 0.004, and 0.001, correspondingly.

3.6. Analytical applications

The suggested method was employed to assess zinc concentrations in a collection of samples, which included various food items and milk products. The system operated using the refined parameters listed in Table 2. Table 4 presents the outcomes obtained from the analyzed samples. To evaluate accuracy, these results were compared with those acquired through FAAS. A paired *t*-test and *F*-test[64] were applied, revealing no statistically substantial differences at the 95% confidence interval. To showcase the effectiveness of the developed system, the outlined procedure was utilized for the analysis of Zn^{2+} ions in different water sources, like river, seawater, well, tap, and wastewater. The method's accuracy was validated through recovery tests and by comparing the obtained results with those from FAAS. The findings are presented in Table 5.

The developed technique was effectively utilized to quantify zinc in pharmaceutical products. Its precision was confirmed by contrasting the findings with that of the FAAS technique (Table 6). The developed technique was tested for efficiency using the *t*-test to evaluate precision and the *F*-test to examine precision, with comparisons made against FAAS. Mean values were calculated using Student's *t*-test and the *F*-statistic at a 95% confidence interval with five degrees of freedom.[64] The findings revealed that the computed values (Table 6) remained below the expected theoretical limits.

To assess the method's reliability, it was implemented across multiple scenarios. Various human serum specimens were examined for this evaluation. A statistical comparison was conducted against results obtained through FAAS, revealing

Table 5 Measurement of zinc concentrations in various water samples

Sample	Added ($ng\ mL^{-1}$)	Found[a] ($ng\ mL^{-1}$)	Recovery (%)	FAAS[a] ($ng\ mL^{-1}$)	*t*-Test[b]	*F*-Value[c]
Tap water[d]	—	2.3 ± 0.1[g]	—	2.3 ± 0.2[g]		
	75.0	78.0 ± 0.1	100.91	76.5 ± 0.3	1.55	
	150.0	151.5 ± 0.2	99.47	12.1 ± 0.4		3.23
River water[e]	—	10.5 ± 0.3	—	10.4 ± 0.8		
	125.0	134.0 ± 0.2	98.89	137.5 ± 0.7		3.59
	250.0	265.5 ± 0.4	101.92	257.5 ± 0.6	1.67	
Sea water[f]	—	15.5 ± 0.3	—	15.5 ± 0.5		
	200.0	213.0 ± 0.2	98.84	219.0 ± 0.9	1.42	
	400.0	420.5 ± 0.3	101.20	408.0 ± 1.2		3.05
Well water[d]	—	7.6 ± 0.1	—	7.5 ± 0.2[g]		
	250.0	261.0 ± 0.2	101.32	252.0 ± 0.2		3.73
	500.0	501.5 ± 0.2	98.80	515.0 ± 0.2	1.57	
Waste water[c]	—	72.5 ± 0.3	—	72.7 ± 2.3		
	225.0	300.5 ± 0.6	101.01	295.0 ± 0.9	1.28	
	450.0	520.0 ± 0.2	99.52	527.0 ± 1.2		2.87

[a] Averages ± standard deviations of six determinations. [b] The critical *t*-value ($\alpha = 0.05$, df = 5) = 2.57. [c] The critical *F*-value ($\alpha = 0.05$, df = 5) = 5.05. [d] Collected from Zagazig, Egypt. [e] Collected from Benha, Egypt. [f] Collected from Alexandria, Egypt. [g] After preconcentration.

Table 6 Analysis of pharmaceutical formulations

Sample	Certified value	Zinc found[a]		t-Test[b]	F-Value[c]
		Proposed	FAAS		
Prozoline zinc (solution)[d]	10.1 mg/10 mL	10.1 ± 0.05	10.3 ± 0.12	1.83	3.79
Vita zinc (capsules)[e]	25.0 mg per capsule	24.6 ± 0.04	24.5 ± 0.11	1.56	3.38
Hamoderme (talc powder)[f]	243 mg g^{-1}	241.5 ± 0.05	241.0 ± 0.14	1.91	4.15
Stresstabs* 600[g]	9.67 mg per capsule	9.65 ± 0.06	9.70 ± 0.17	1.74	3.63

[a] Means ± standard deviations. [b] The critical t-value ($\alpha = 0.05$, df = 5) = 2.57. [c] The critical F-value ($\alpha = 0.05$, df = 5) = 5.05. [d] Produced by Kahira Pharmaceutical and Chemical Industrial, each 100 mL includes 2.0 mg of cetrimide, 50 mg of maleate, 50 mg of naphazoline HCl, and 250 mg of zinc sulfate. [e] Produced by Medical Union Pharmaceutical in Abuo-Sultan, Egypt, this product includes 23.9 mg of zinc sulfate, 10 mg of pyridoxine HCl, 10 mg of riboflavin, 100 mg of nicotinamide, 20 mg of thiamine monohydrate, 25 mg of cyanocobalamin, 25 mg of calcium pantothenate, and 3.0 mg of cupric oxide. [f] Produced by Nile Company for Pharmaceutical and Chemical Industry, Cairo, Egypt. Each 100 g includes: 30 g zinc oxide, 2.0 g camphor, 0.5 g zinc sulfate, 1.0 g copper sulfate, and 66.5 g purified talc. [g] Produced by the Egyptian International Pharmaceutical Industries Company (EIPICO), Egypt, this product includes 175 mg of zinc gluconate, 50 000 IU of vitamin A, and 100 mg of vitamin E.

Table 7 Determination of zinc in human serum samples using proposed and FAAS methods ($n = 5$)[a]

Sample	Added (μg mL^{-1})	Found[b] (μg mL^{-1})		t-Test[c]	F-Value[d]
		PM	FAAS		
Human serum 1	—	1.50 ± 0.3	1.45 ± 1.2		
	1.50	3.50 ± 0.4	2.90 ± 1.5	1.81	3.97
	3.00	4.40 ± 0.2	4.55 ± 1.3	1.47	3.15
Human serum 2	—	2.75 ± 0.4	2.80 ± 1.1		
	2.00	4.80 ± 0.3	4.90 ± 0.6	1.96	4.16
	4.00	6.85 ± 0.5	6.70 ± 0.9	1.32	2.98
Humanserum 3	—	1.70 ± 0.3	1.75 ± 1.9		
	0.50	2.30 ± 0.4	2.20 ± 1.8	1.88	4.02
	1.00	2.80 ± 0.5	2.65 ± 1.5	1.36	2.97
Human serum 4	—	2.40 ± 0.4	2.45 ± 1.6		
	1.00	3.35 ± 0.3	3.55 ± 2.8	1.72	3.57
	2.00	4.50 ± 0.5	4.35 ± 1.5	1.53	3.22

[a] PM, proposed method. [b] Averages ± standard deviations of six determinations. [c] The critical t-value ($\alpha = 0.05$, df = 5) = 2.57. [d] The critical F-value ($\alpha = 0.05$, df = 5) = 5.05.

a strong level of consistency. The corresponding data are presented in Table 7. The suggested approach yielded acceptable mean recovery rates and demonstrated strong concordance with the results obtained *via* FAAS in a variety of biological specimens. The findings attained from certain biological samples using this method were statistically relative to those acquired through the FAAS method (Table 8). Based on the statistical indicators presented in Table 8, including the F-value and Student's t-test, it can be concluded that the technique demonstrates similar levels of accuracy and precision. Alternatively, the proposed method can serve as a routine analytical technique replacing the FAAS approach. Due to its enhanced sensitivity compared to FAAS, this method is particularly beneficial for detecting low levels of zinc. To assess its performance, the proposed procedure was tested across various scenarios, including the analysis of multiple human serum samples.

Table 8 Zinc levels in certain biological samples following the application of proposed and FAAS methods ($n = 5$)

Sample	Concentration (μg g^{-1})		RSD (%)	t-Test[a]	F-Value[b]
	FAAS	PM			
Feces	4940 ± 20	4935 ± 30	1.15	1.18	2.71
Saliva[c]	49.5 ± 1.7	49.0 ± 1.6	0.86	1.11	2.66
Femur	183.0 ± 4.0	184.5 ± 2.0	1.04	1.04	2.47
Kidney	26.0 ± 2.0	27.0 ± 1.0	1.28	1.21	2.86
Urine[c]	52.0 ± 1.6	51.0 ± 1.9	0.98	0.84	2.26
Human hair	82.0 ± 1.8	82.5 ± 2.7	1.07	1.77	2.43

[a] The critical t-value ($\alpha = 0.05$, df = 5) = 2.57. [b] The critical F-value ($\alpha = 0.05$, df = 5) = 5.05. [c] μg per Zn^{2+}L.

4 Conclusions

The present method is distinguished by the subsequent features:

(1) AHDDO is an increasingly sensitive and selective spectrophotometric reagent for zinc quantification, known for its ease of preparation and high purity. The zinc complex exhibits an exceptionally high molar absorptivity, reaching up to 9.78 × 10^7 L mol^{-1} cm^{-1} using a 1000 mL sample.

(2) Higher sample volumes lead to greater sensitivity. The quantification and detection limits attained 50 and 15 ng mL^{-1}

for 500 mL sample, while for 1000 mL sample they were 20 and 6.0 ng mL^{-1}, correspondingly, when using 50 mg of Dowex 1-X8.

(3) Zinc determination remains largely unaffected by most extraneous ions. Interference of Cu^{2+} is effectively eliminated by employing 1.0 mL of 0.3% oxalate solution as masking agent whereas for Cd^{2+} is prevented employing 1.0 mL of 0.5% thiocyanate solution, which increases the tolerance limit by 500-fold excess.

(4) Effective implementation of the described technique for detecting ultra-trace Zn amounts in a variety of environmental food samples, water, pharmaceutical dosage forms, serum, urine and some biological samples employing the standard additions technique was performed with good findings compared to the FAAS procedure.

Ethical approval

All animal procedures were performed in accordance with the Guidelines for Care and Use of Laboratory Animals of the Zoology Department, Faculty of Science, Benha University and approved by the Animal Ethics Committee of the World Organization for Animal Health. All experiments were performed in accordance with the Guidelines of the Laboratory Animal Ethics Committee of Egypt, and experiments were approved by the ethics committee at the Ethics of Scientific Research, Faculty of Medicine, Benha University (specify the approval number: FSC No. 295-25). Informed consents were obtained from human participants of this study.

Author contributions

Fahad Alminderej, Muneera Alrasheedi and Alaa Younis: conceptualization, data curation, investigation. Supervision, writing – review. Alaa Amin and Hesham El-Feky: conceptualization, methodology, data curation, investigation, supervision, validation, writing – original draft, writing – review & editing.

Conflicts of interest

Authors have no conflicts of interest to declare.

Data availability

The authors declare that the data supporting the findings of this study are available within the article.

Acknowledgements

The authors' sincere thanks are due to Qassim and Benha Universities, for providing the necessary facilities.

References

1 Y. Chen, X. Wang, J. Zhou, G. Wang, T. Gao, H. Wei, Y. Che, T. Li, Z. Zhang, S. Wang, L. Hu and R. Lu, *Ecotoxicol. Environ. Saf.*, 2024, **284**, 116889.
2 P. Deng, X. Han, J. Ma, X. Huang, B. Sun, Y. Geng, B. Zheng and S. Wang, *BioMetals*, 2022, **35**, 955–965.
3 J. Burgess and R. H. Prince, Zinc: inorganic & coordination chemistry, in *Encyclopedia of Inorganic Chemistry*, Wiley, 2005.
4 S. Chia, C. Ong, L. Chua, L. Ho and S. Tay, *J. Androl.*, 2000, **21**, 53–57.
5 T. Das, A. Ammal, A. Harshey, V. Mishra and A. Srivastava, *Microchem. J.*, 2021, **171**, 106810.
6 J. E. Allard, G. Davidson, A. Baird, M. Boyce, S. Jones, J. Lewis, C. Lowrie and B. M. McBride, *Sci. Justice*, 2023, **63**, 477–484.
7 B. Singh, I. Gautam, V. K. Yadav and B. K. Mohapatra, *Eur. J. Forensic Sci.*, 2015, **2**, 14–18.
8 A. Stroud, A. Gamblin, P. Birchall, S. Harbison and S. Opperman, *Sci. Justice*, 2023, **63**, 414–420.
9 V. Sharma, M. Sahu, A. K. Manna, D. De and G. K. Patra, *RSC Adv.*, 2022, **12**, 34226–34235.
10 M. A. El-Bindary, A. Shahat, I. M. El-Deen, M. A. Khalil and N. Hassan, *Desalin. Water Treat.*, 2022, **274**, 261–277.
11 K. J. Gosnell, W. M. Landing and A. Milne, *Mar. Chem.*, 2012, **132**, 68–76.
12 O. Wada, *Asian Med. J.*, 2004, **47**, 351–358.
13 M. K. Goshisht, G. K. Patra and N. Tripathi, *Adv. Mater.*, 2022, **3**, 2612–2669.
14 W. Abd El-Fattah, A. Guesmi, N. Ben Hamadi, M. A. Khalil and A. Shahat, *Appl. Organomet. Chem.*, 2024, **38**, e7407.
15 M. Rezaee and P. Tajer-Mohammad-Ghazvini, *Bull. Chem. Soc. Ethiop.*, 2022, **36**, 1–11.
16 N. I. H. National Institutes of Health, Zinc – Fact Sheet for Health Professionals, 2022, available at: **https://ods.od.nih.gov/factsheets/Zinc-HealthProfessional/**.
17 K. R. Wessels and K. H. Brown, *PLoS One*, 2012, **7**, e50568.
18 M. Knez and C. R. Stangoulis, *Nutr. Res. Rev.*, 2023, **36**, 199–215.
19 N. M. Lowe, A. G. Hall, M. R. Broadley, J. Foley, E. Boy and Z. A. Bhutta, *Adv. Nutr.*, 2024, **15**, 100181.
20 A. G. Hall, J. C. King and C. M. McDonald, *Biol. Trace Elem. Res.*, 2022, **200**, 2606–2613.
21 Z. Wang, X. Wang, Q. Wang, X. Xiong, H. Luo and K. Huang, *Microchem. J.*, 2019, **149**, 104052.
22 O. M. A. Shahlol, K. I. Salem and S. N. Alkateb, *Surman J. Sci. & Tech.*, 2025, **7**, 145–155.
23 S. Sultana, H. A. Khatun, M. Faruquee, M. M. Ul Islam, H. J. Tonny and M. R. Islam, *Foods*, 2023, **12**, 1044.
24 N. Bithi, D. Ricks, B. S. Walker, C. Law and K. L. Johnson-Davis, *J. Mass Spectrom. Adv. Clin. Lab*, 2024, **34**, 21–27.
25 O. Zverina, M. Vychytilova, J. Rieger and W. Goessler, *Spectrochim. Acta B*, 2023, **201**, 106616.
26 M. Shamsipur, T. Poursaberi, M. Hassanisadi, M. Rezapour, F. Nourmoham madian and K. L. Alizadeh, *Sens. Actuators B-Chem.*, 2012, **161**, 1080–1087.
27 S. Yousefi, S. Makarem, W. Alahmad, F. D. Zare and H. Tabani, *Talanta*, 2022, **238**, 123031.
28 W. Abd El-Fattah, A. Guesmi, N. Ben Hamadi, M. A. Khalil and A. Shahat, *Appl. Organomet. Chem.*, 2024, **38**, 7407.

29 H. Li, J. Zhao, S. Zhao and G. Cui, *Microchem. J.*, 2021, **168**, 106390.
30 S. H. Sutheimer and S. E. Cabaniss, *Anal. Chim. Acta*, 1995, **303**, 211–221.
31 M. Ahmed and R. Narayanaswamy, *Sci. Total Environ.*, 1995, **163**, 211–227.
32 P. T. Anastas, *Crit. Rev. Anal. Chem.*, 1999, **2**, 167–175.
33 P. Tundo and T. C. Williamson, *Green Chemistry: Challenging and Perspectives*, Oxford University Press, 1998.
34 M. T. Stack and A. M. Golichowski, *Electrophoresis*, 1981, **2**, 307–314.
35 A. S. Amin and A. A. Gouda, *Talanta*, 2008, **76**, 1241–1245.
36 H. Waki, *Ion Exchange and Solvent Extraction*, CRC Press, 2021, pp. 197–228.
37 A. S. Amin and M. A. Kassem, *Spectrochim. Acta A*, 2012, **96**, 541–547.
38 A. S. Amin, A. M. El-Sharjawy and M. A. Kassem, *Spectrochim. Acta A*, 2013, **110**, 262–268.
39 L. S. G. Teixeira, F. R. P. Rocha, M. Korn, B. F. Reis, S. L. C. Ferreira and A. C. S. Costa, *Anal. Chim. Acta*, 1999, **383**, 309–315.
40 M. Benamor, K. Belhamel and M. T. Draa, *J. Pharm. Biomed. Anal.*, 2000, **23**, 1033–1038.
41 S. Zhivkova, K. Dimitrov, G. Kyuchoukov and L. Boyadzhiev, *Sep. Purif. Technol.*, 2004, **37**, 9–16.
42 A. Molina-Diaz, J. F. Garcia-Reyes and B. Gilbert-Lopez, *Trends Anal. Chem.*, 2010, **29**, 654–666.
43 J. J. B. Nevado, J. A. M. Leyva and M. R. Ceba, *Talanta*, 1976, **23**, 257–258.
44 K. J. Reddy, J. R. Kumar, C. Ramachandraiah, T. Thriveni and A. V. Reddy, *Food Chem.*, 2007, **101**, 585–591.
45 M. F. Molina, M. Nechar and J. M. Bosque-Sendra, *Anal. Sci.*, 1998, **14**, 791–797.
46 M. A. Herrador, A. M. Jimenez and A. G. Asuero, *Analyst*, 1987, **112**, 1237–1246.
47 K. Yoshimura, H. Waki and S. Ohashi, *Talanta*, 1978, **25**, 579–583.
48 I. C. Santos, R. B. R. Mesquita and A. O. S. S. Rangel, *Anal. Chim. Acta*, 2015, **891**, 171–178.
49 A. S. Amin, *Anal. Biochem.*, 2011, **418**, 172–179.
50 M. J. Ayora-Canada, M. I. Pascual-Reguera and A. Molina-Doaz, *Anal. Chim. Acta*, 1998, **375**, 71–80.
51 L. S. G. Teixeira, F. R. P. Rocha, M. Korn, B. F. Reis, S. L. C. Ferreira and A. C. S. Costa, *Talanta*, 2000, **51**, 1027–1033.
52 M. I. Tora, N. Lara, J. Narváe and P. Richte, *J. Chil. Chem. Soc.*, 2004, **49**, 163–168.
53 J. Vukovic, S. Matsuoka, K. Yoshimura, V. Grdinic, R. J. Grubesic and O. Zupanic, *Talanta*, 2007, **71**, 2085–2091.
54 K. Yoshimura, H. Waki and S. Ohashi, *Talanta*, 1976, **23**, 449–454.
55 A. O. S. Bahathiq, A. O. Babalghith, A. S. Amin and A. M. Askar, *Environ. Sci.: Adv.*, 2024, **3**, 776–788.
56 G. Schwarzenbach, H. Flaschka and H. Irving, *Complexometric Titrations*, Methuen, London, 2nd edn, 1969, pp. 260–268.
57 A. S. Amin and Y. M. Issa, *Mikrochim. Acta*, 2000, **134**, 133–138.
58 A. Molina-Diaz, J. M. Herrador-Mariscal, M. I. Pascual Reguera and L. F. Capitan-Vallvey, *Talanta*, 1993, **40**, 1059–1066.
59 M. L. Fermindez-de Cdrdova, A. Molina-Diaz, M. I. Pascual-Reguera and L. F. Capitfin-Vallvey, *Talanta*, 1995, **42**, 1057–1065.
60 K. Yoshimura and S. Ohashi, *Talanta*, 1978, **25**, 103–107.
61 M. R. Baezzat and M. Karimi, *Int. J. ChemTech Res.*, 2013, **5**, 2503–2507.
62 H. Tavallali and Y. Mozhdeh, *Eurasian J. Anal. Chem.*, 2008, **3**, 3–8.
63 IUPAC, Data interpretation, *Spectrochim. Acta B*, 1978, **33**, 241–245.
64 J. N. Miller and J. C. Miller, *Statistics and Chemometrics for Analytical Chemistry*, Prentice-Hall, London, 5th edn, 2005.